

Neutron measurements of the single-particle kinetic energies in solid neon

D. N. Timms*

Division of Physics, School of Earth and Environmental Sciences, Portsmouth University, Portsmouth PO1 3QL, United Kingdom

R. O. Simmons

Frederick Seitz Materials Research Laboratory and Department of Physics, University of Illinois at Urbana-Champaign, Urbana, Illinois 61801-3080

J. Mayers

ISIS Facility, Rutherford Appleton Laboratory, Chilton, Didcot OX11 0QX, United Kingdom

(Received 16 October 2002; revised manuscript received 6 February 2003; published 1 May 2003)

Direct measurements of the mean atomic kinetic energy of solid neon have been made at 16 temperatures in the range 5–22 K and saturated vapor pressure. The measurements were made at high momentum and energy transfers using the technique of neutron Compton scattering. These extensive data have been compared with published calculations, and there is general agreement. The ground-state kinetic energy in condensed neon has been determined to be 41(2) K.

DOI: 10.1103/PhysRevB.67.172301

PACS number(s): 63.20.–e, 61.12.Ex, 67.80.Cx

For a classical system such as krypton or xenon $n(\mathbf{p})$ is given by a Maxwell-Boltzmann distribution, and it is Gaussian with a width determined by the mean single-particle kinetic energy, $\langle E_k \rangle$. Near melting, $\langle E_k \rangle$ is given by classical equipartition.¹ For the more massive inert gases the zero-point energy, which is inversely proportional to the atomic mass, is small and plays a minor role in shaping their physical properties. However, the strong quantum interactions in helium result in significant deviations from this Gaussian behavior, making it the subject of many detailed investigations.² Solid neon is an intermediate system. The shape of $n(\mathbf{p})$ is Gaussian but quantum effects are manifest as an excess in the measured values of $\langle E_k \rangle$ above the classical prediction and the existence of a significant zero-point energy.³

In a previous study⁴ of the kinetic energy in solid neon we reported results which were broadly in agreement with path-integral Monte Carlo (PIMC) calculations performed using both modified Hartree-Fock dispersion (HFD-C2) and Lennard-Jones (LJ) pair potentials. This experiment was performed at very high energy and momentum transfers, where the validity of the impulse approximation (IA) was assured and corrections for final-state effects were unnecessary. The results obtained were significantly lower than those of previous measurements³ and were used to support the PIMC method over the Wigner-Kirkwood expansion method performed with the same two pair potentials. It was also shown that the computed kinetic energy is not critically dependent on the model pair potential chosen, with the HFD-C2 yielding slightly lower values.

Our motivation for the present work was the publication of additional calculations.^{5,6} Existing experimental data are in broad agreement with these new calculations but are limited to just a few isolated temperatures. These data were unable either to confirm the predicted temperature dependence or to estimate the ground state $\langle E_k \rangle$ with confidence. In this paper we report systematic, high-precision measure-

ments of $\langle E_k \rangle$ of solid neon between 5 and 22 K at mostly 1° intervals of temperature. Further, as this paper was written, independent PIMC work was published,⁷ which also shows that $\langle E_k \rangle$ values computed using an HFD potential are slightly smaller than those using a LJ potential.

Neutron Compton scattering (NCS) is the neutron analog of photon Compton scattering and measures the atomic momentum distribution $n(\mathbf{p})$. It is a neutron-scattering technique made possible by the construction of accelerator-based sources such as the ISIS facility, United Kingdom. The momentum of a particle is a fundamental concept in both classical and quantum mechanics and the Vesuvio electron volt spectrometer (eVS) at ISIS is the leading instrument designed to accurately measure atomic momentum distributions, $n(\mathbf{p})$, in condensed matter.⁸ The high-energy and momentum transfers available with eVS ensure that the interaction between the neutron and target atom is well approximated by the IA. In the IA, the struck atom is assumed to recoil freely and interatomic interactions in the final state are negligible.⁹ The quantity measured in NCS experiments is the longitudinal momentum distribution or neutron Compton profile, $J(y)$, and the width of $J(y)$ provides a direct measurement of $\langle E_k \rangle$. Details of the Vesuvio eVS and the data analysis procedure used here can be found elsewhere.^{4,8} Another method, using Doppler broadening from resonant nuclear reactions, still is not competitive for determining $n(\mathbf{p})$ in neon.¹⁰

Natural neon samples of volume 16 cm³ were contained within a square-sided aluminum can of thickness 10 mm. Boron nitride shielding was used to limit the range of potential scattering angles viewed by any one detector. This shielding proved very successful in limiting the effects of multiple scattering in this large sample. The remaining multiple-scattering contribution was estimated by Monte Carlo simulation and then removed from the time-of-flight (TOF) spectrum. The cell temperatures were maintained to within 0.1° in the sample space of an “orange” cryostat.

TABLE I. Values for the kinetic energy of various solid neon samples obtained by both experimental measurements and PIMC calculations. Present experimental values were taken at high Q , in the impulse approximation regime, as were those of Ref. 7.

T (K)	ρ (nm^{-3})	Experiment $\langle E_k(\rho, T) \rangle$ (K)	Reference	T (K)	ρ (nm^{-3})	Calculations $\langle E_k(\rho, T) \rangle$ (K)	Reference
4.25(5)	44.97	44.0(10)	4	4.125	44.97	41.6(1)	4(HFD)
4.7(1)	44.97	49.2(28)	3	4.7	44.97	41.2(11)	7(HFD)
5.0(1)	44.97	42.5(8)	present	5.0	^a	41.7(1)	5(LJ)
7.0(1)	44.94	43.0(9)	present				
8.0(1)	44.92	41.7(9)	present				
8(2)		37(7) ^b	10				
9.0(1)	44.89	42.4(9)	present				
9.4(1)	44.87	49.1(40)	3	9.4	44.87	41.9(3)	7(HFD)
10.0(1)	44.85	43.7(8)	present	10.0	^a	42.5(1)	5(LJ)
				10.154	44.85	42.6(1)	4(HFD)
10.2(1)	44.84	43.0(10)	4	10.2	44.68	41.8(3)	7(HFD)
11.0(1)	44.80	43.2(9)	present				
11.4(2)	44.77	49.0(24)	3	11.4	44.77	42.5(2)	7(HFD)
12.0(1)	44.74	42.6(9)	present	12.0	^a	43.2(1)	5(LJ)
13.0(1)	44.66	43.3(9)	present				
14.0(1)	44.57	43.4(9)	present				
15.0(1)	44.47	43.4(9)	present	15.0	^a	44.6(1)	5(LJ)
16.0(1)	44.35	45.4(9)	present	15.687	44.48	46.5(1)	4(HFD)
17.0(1)	44.23	44.5(9)	present	17.0	^a	45.1(1)	5(LJ)
17.8(2)	44.12	51.2(28)	3	17.8	44.12	45.9(1)	7(HFD)
18.0(1)	44.08	44.3(9)	present				
19.0(1)	43.93	44.4(9)	present				
20.0(1)	43.75	47.1(9)	present	20.0	^a	48.0(1)	5(LJ)
20.2(1)	43.74	48.0(10)	4	20.2	43.91	47.9(2)	7(HFD)
				20.308	43.50	47.8(1)	4(HFD)
22.0(1)	43.35	47.6(10)	present				
26.4(2)	43.26	57.9(20)	3	26.4	43.26	54.1(1)	7(HFD)

^aAdjusted “zero-pressure” densities (see text).

^bIncludes possible surface effect.

Temperature sensors and heaters were positioned at the top and bottom of the sample to maintain a minimum-temperature gradient across the sample. The neon samples were prepared by filling through a vertical capillary of 0.5-mm i.d. connected to pressure gauges and a ballast volume of about 1 liter all at room temperature. The observed pressure changed little throughout the experiment, implying that a relatively constant level of liquid neon was maintained in the capillary. The solid neon sample was prepared by first liquefying the sample and then cooling the sample until it solidified. At a long TOF ($>2000 \mu\text{s}$), the eVS spectra show peaks arising from neutron diffraction within the sample and these peaks were used to confirm the polycrystalline nature of the sample. Good agreement at all temperatures, between the observed lattice parameters and those expected,¹¹ indicates both that the sample temperatures are accurately known and that the sample was not constrained within the cell. For each sample approximately 4 h of run time was used. The sample was then cooled to a new temperature and left for 1 h to reach thermal equilibrium

before continuing with the measurements.

Analysis of the data was performed by fitting in time of flight; the details of this procedure can be found elsewhere.⁸ Only the dominant ^{20}Ne scattering was retained for analysis; the other isotope contributions were removed using the procedure outlined in Timms *et al.*⁴ The mean atomic kinetic energy was obtained by fitting the 32 recoil spectra obtained at each temperature with a Voigt resolution function convoluted with the Gaussian momentum distribution (see Timms *et al.*⁴ and Andreani *et al.*¹² for details) and the mean atomic kinetic energy $\langle E_k \rangle$ was determined from the Gaussian width. At the large momentum transfers used here ($Q > 750 \text{ nm}^{-1}$) corrections for final-state effects (FSE) are unnecessary and the values of $\langle E_k \rangle$ listed in the table are without FSE correction.

Values for $\langle E_k \rangle$ of solid neon obtained by both experimental measurement and recent PIMC calculations are given in Table I. Note that these may apply to somewhat different conditions. The present work applies to ^{20}Ne . The nuclear resonance data¹⁰ were taken on ^{21}Ne . Among the PIMC cal-

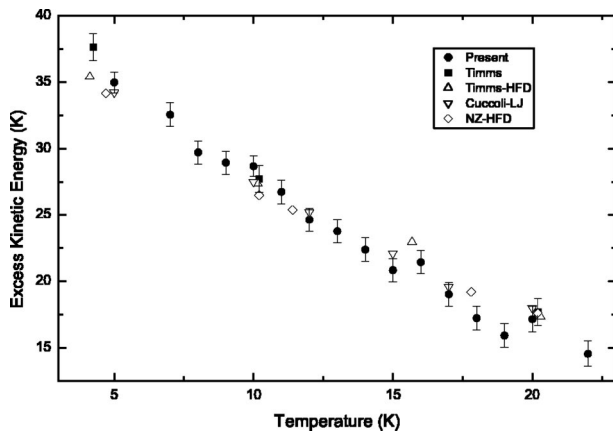


FIG. 1. Kinetic-energy excess above $(3/2)k_B T$ in solid neon as a function of temperature. (●), present data; (■) and (△), experimental measurements and PIMC calculations, respectively, from Timms *et al.* (Ref. 4); (▽) and (◇), PIMC calculations by Cuccoli *et al.* (Ref. 5) and by Neumann and Zoppi (Ref. 7), respectively.

culations, those of Timms *et al.*⁴ were for mass 20 amu, those of Neumann and Zoppi⁷ were for mass 20.184 amu, at the specified densities, and those of Cuccoli *et al.*⁵ were for “neon” and the density is unspecified except through the statements “. . . density was adjusted in such a way as to get a practically vanishing pressure. . . zero-pressure densities turned out to be very close to the experimental ones.”

The temperature dependence of the kinetic-energy excess above the classical equipartition value is shown in Fig. 1. Previous eVS measurements⁴ are of precision similar to the present ones, but are limited to just three temperatures, making an accurate estimate of the zero-point energy difficult. The figure shows agreement between our present data and these earlier results, and the increased density of present data points allows the zero-point energy to be determined from data points below 10 K as 41(2) K. The figure also shows that the theoretically predicted temperature dependence of $\langle E_k \rangle$ is observed. Agreement is also evident between the new PIMC calculations^{5,7} and those presented in our previous study.⁴

Present NCS spectra show the total scattering for all neon isotopes, but the recoil spectra overlap and are of insufficient precision to distinguish possible differences between $\langle E_k \rangle$ for different isotopes. We note that PIMC methods have been extended to study thermal expansion of neon isotopes,¹³ and the results on a relative basis show agreement with anomalies at high temperature first demonstrated by experiment.¹⁴ Results for relative isotopic $\langle E_k \rangle$ values are not given, however.

Acocella *et al.* have used the improved effective potential Monte Carlo and improved self-consistent theories to study the thermal and elastic properties of solid neon.¹⁵ Such calculations, unlike a PIMC simulation which uses an experimentally given density, pass the more demanding test of precisely obtaining the equilibrium density owing to equilibrium thermal expansion. These authors conclude that although their realistic potential is the best currently available, it is not significantly superior to a suitably chosen nearest-neighbor Lennard-Jones potential in their calculations. Their Table I lists a calculated zero-point energy of 77.94 K, from which a harmonic division would yield 39.0 K for the kinetic energy. Presumably, however, strictly harmonic division is not appropriate, because of known anharmonicity in solid neon. Unfortunately, kinetic energies versus temperature are not given.

Traditional thermodynamic tests of lattice-dynamics models rely on comparisons with experiment of derivatives of the free energy, such as temperature dependence of the lattice parameter,^{11,14} bulk modulus,¹¹ and internal energy.¹⁶ To those scalar quantities one can now usefully add the kinetic energy.

This research was supported by the UK EPSRC with the provision of beam time. R.O.S. was supported by the US DOE, Division of Materials Sciences, Contract No. DEFG02-91ER445439. We are grateful to J. Dreyer, I. F. Bailey, J. Bones, and other technical staff from the ISIS facility, Rutherford Appleton Laboratory, for their assistance with these measurements. We are also grateful to A. Cuccoli for making the results of his PIMC simulations available to us before their publication.

*Electronic address: david.timms@port.ac.uk

¹D.A. Peek and R.O. Simmons, *J. Chem. Phys.* **94**, 3169 (1991).

²See, for example, R.O. Hilleke, P. Chaddah, R.O. Simmons, D.L. Price, and S.K. Sinha, *Phys. Rev. Lett.* **52**, 847 (1984); H.A. Mook, *Phys. Rev. B* **37**, 5806 (1988); W.M. Snow, Y. Yang, and P.E. Sokol, *Europhys. Lett.* **19**, 403 (1992); K.H. Anderson, W.G. Stirling, A.D. Taylor, S.M. Bennington, Z.A. Bowden, I. Bailey, and H.R. Glyde, *Physica B* **181**, 865 (1992); R.C. Bladwell, D.M. Ceperley, and R.O. Simmons, *Z. Naturforsch., A: Phys. Sci.* **48**, 433 (1993); R.T. Azuah, W.G. Stirling, K. Guckelsberger, R. Scherm, H.R. Glyde, S.M. Bennington, and A.D. Taylor, *Physica B* **213-214**, 454 (1995); D.M. Ceperley, R.O. Simmons, and R.C. Bladwell, *Phys. Rev. Lett.* **77**, 115 (1996); M. Celli, M. Zoppi, and J. Mayers, *Phys. Rev. B* **58**, 242 (1998).

³D.A. Peek, I. Fujita, M.C. Schmidt, and R.O. Simmons, *Phys. Rev. B* **45**, 9680 (1992).

⁴D.N. Timms, A.C. Evans, M. Boninsegni, D.M. Ceperley, J. Mayers, and R.O. Simmons, *J. Phys.: Condens. Matter* **8**, 6665 (1996).

⁵A. Cuccoli, A. Macchi, G. Pedrolli, V. Tognetti, and R. Vaia, *Phys. Rev. B* **56**, 51 (1997).

⁶M. Asger and Q.N. Usmani, *Physica B* **271**, 104 (1999).

⁷M. Neumann and M. Zoppi, *Phys. Rev. E* **65**, 031203 (2002).

⁸A.C. Evans, J. Mayers, D.N. Timms, and M.J. Cooper, *Z. Naturforsch., A: Phys. Sci.* **48**, 425 (1993), and references therein.

⁹V.F. Sears, *Phys. Rev. A* **5**, 452 (1971); **7**, 340 (1973).

¹⁰M. Berheide, W.H. Schulte, H.-W. Becker, L. Borucki, M. Buschmann, N. Piel, C. Rolfs, G.E. Mitchell, and S. Schweitzer, *Phys. Rev. B* **58**, 11 103 (1998).

- ¹¹D.N. Batchelder, D.L. Losee, and R.O. Simmons, *Phys. Rev.* **162**, 767 (1967).
- ¹²C. Andreani, G. Baciocca, R.S. Holt, and J. Mayers, *Nucl. Instrum. Methods Phys. Res. A* **276**, 297 (1989).
- ¹³M.H. Müeser, P. Nielaba, and K. Binder, *Phys. Rev. B* **51**, 2723 (1995).
- ¹⁴D.N. Batchelder, D.L. Losee, and R.O. Simmons, *Phys. Rev.* **173**, 873 (1968).
- ¹⁵D. Acocella, G.K. Horton, and E.R. Cowley, *Phys. Rev. B* **61**, 8753 (2000).
- ¹⁶E. Somoza and H. Fenichel, *Phys. Rev. B* **3**, 343 (1971).